



Optical band gap, surface and grain size behaviours of Cu 90%-Al₂O₃10% wt alloy nanoparticles by high energy ball milling

G Kesavana¹, Dr. A Christy Ferdinand², Dr. D Manikandanc³

¹ Research Scholar, Department of Physics, St. Joseph's College of Arts and Science (Autonomous) Cuddalore, Tamil Nadu, India

² Assistant Professor, Department of Physics, Periyar Govt Arts and Science College, Cuddalore, Tamil Nadu, India

³ Assistant Professor, Department of Physics, Arignar Anna Govt Arts and Science College Villupuram, Tamil Nadu, India

Abstract

In the present investigation on the preparation of CuO doped Al₂O₃ nanoparticles using high energy ball-milling. Copper oxide (CuO) belongs to the monoclinic crystal system, aluminium oxide (Al₂O₃) belongs to the trigonal crystal system. Copper oxide is low melting and boiling point to compare aluminium oxide. CuO 90%- Al₂O₃ 10% doped new alloy prepared by ball milling technique and heat treatment for furnace in 500°C. The CuO-Al₂O₃ doped nano-materials characterized by UV-visible spectroscopy for optical band gap, SEM for the surface and X-RD to calculate the crystalline size and the lattice distortion.

Keywords: nanoparticles, high energy ball-milling, CuO-Al₂O₃, UV, X-RD, SEM

Introduction

Superconductors for efficient in modern material science. Alternative to the superconductor material for an electrical properties ensure to reduce the loss of electricity. In the transmission process is consumes use part electricity that produced in high investment. Aluminium as very high efficient in transmittance electricity but it has also a drawback of losing its tensile strength it can possess such high mechanical craft property in order to overcome its disadvantage copper as on such a pearlier property so, alloying Cu-Al material can have a distinct future material^[4]. Various type of method used to the particle size reduce for chemical vapour deposition, sol-gel Process, ball milling process, electro deposition process and etc. ^[2]. Ball milling process is best to particle size reducing Method. High level heat treatment is one of the easy method for breaks to particles ^[1, 3]. That same time high energy ball milling used in this particle reduced size is nano scale and quantum scale level. Quantum dot scale (1-10) nm, quantum wire scale (1-100) nm, Quantum walls scale (100-1000)nm quantum wires and quantum walls used to nano electronic devices.

Copper oxide (CuO) belongs to the monoclinic crystal system, aluminium oxide (Al₂O₃) belongs to the trigonal crystal system. Copper oxide is low melting and boiling point to compare aluminum oxide. CuO 90%- Al₂O₃ 10% doped new alloy prepared by ball milling technique and heat treatment for furnace in 500°C. The Cu-Al doped nanomaterials characterized by UV-visible spectroscopy for optical properties, SEM for the surface and X- RD to calculate the crystalline size and the lattice distortion ^[1].

Materials and Methods

Experimental Procedure

CuAl powder was synthesized by the solid state reaction

method using copper oxide (CuO) 90% and aluminium oxide (10%) as starting materials is stoichiometric composition. i.e. ratio between the copper oxide and aluminium oxide is9:1

After mixing the compounds are divided into three equal parts for three different experimental works. From that one part of compound is annealed through muff ale furnace for 500° C about 1 hr and then the grind same sample was high energy ball milling for 1 hr at 250 rpm. The next part of compound is first grind by high energy ball milling for 1 hr at 250 rpm and then which brought under muff ale furnace for heat treatment at 500°C about 1 hr. the last part of the compound was only annealed for 1 hr at 500°C thus the above three different kinds of treated sample gone under four types of characterization Studies.

X-Ray Diffraction Studies

The fresh as well as milled Cu-Al powder was characterized with an X-Ray Diffractometer was used to investigate the structural changes and phase transformations of powders occur during mechanical milling. Sample preparation of XRD is done as per the standard practice. Sample packing was carried out by filling the Cu-Al powder on a glass slit. Precautions were taken to have a tight powder packing on the glass slit and no manual contamination with the powder specimens. The X-ray diffraction measurements were carried out with the help of a Goniometer Cu K α radiation (K α = 1.54056 Å). In this test the sample was in stationary condition, only the arms of the X- ray tube was rotating in the opposite direction up to 90 0 of 2 θ during the test. The samples were scanned in the range from 30 to 900 of 2 θ with a scan rate of 2 0/ min. The analysis was carried out to find out crystallite size, peak height, crystallinity and also amount of induced strains in the milled.

UV-Visible

UV-Vis absorbance and transmission was recorded using UV-Vis spectrophotometer (cary-50) to investigate the lower cutoff of the transmission which is indirect measure of the stoichiometry of the material.

Morphology Studies

Scanning electron microscopy was used in order to evaluate the morphological changes of certain phases observed in the fresh as well as nano structured Cu-Al particles.

Results and Discussions

1. UV-Visible Spectroscopy

Fig 1 shows the uv-visible spectroscopy of Cu-Al annealed milling spectrum. The optical is reliable and accurate analytical procedure for the analysis of this substance. The uv and visible spectroscopy to study the absorbance, transmission and emission of uv –visible light wave length by matter. Also

to measure the uv cut off shift in the absorbance graph of cu-al alloy material. The ball milled nano particles were reported by the optical studies [8].

The absorbance spectrum fig.1 for Cu-Al annealed milling conform the presence of alloy or coreshells structure cu spr peak centered at 550 nm and aluminium spr peak centered at 300 nm.

The Cu-Al noble metals crow with and the uv-cut off is red shifted [6]. This implies that the band gap increase for the Cu-Al nano particles and the band gap accure due to quantum confinement effect.

1.1 Annealed Milling Cu-Al Alloy

Fig.1.1 from the optical spectrum Cu-Al alloy nanomaterials consists two main SPR peaks a sharp peak in the uv region around 316 nm for al nanoclusters move to blue shift and a broad peak in the visible move to red shift around cu 572 nm was observed.

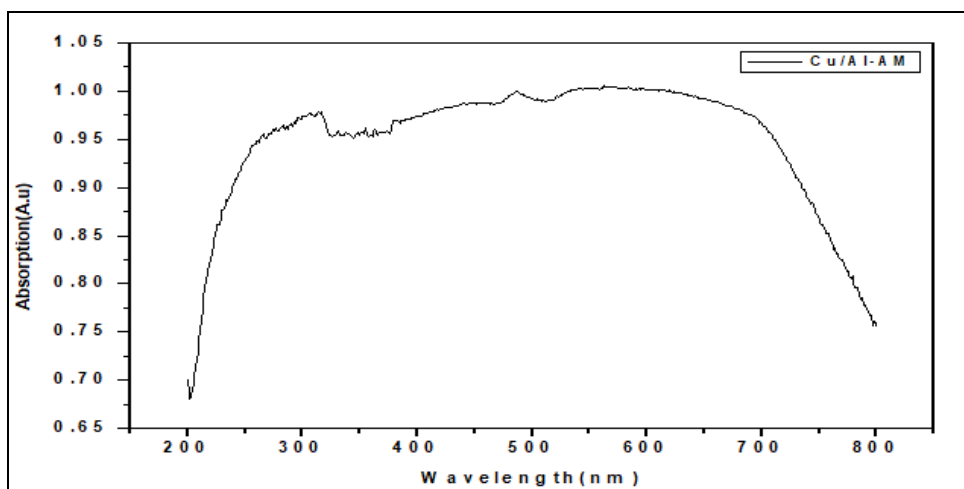


Fig 1.1: Optical absorption spectrum for Cu-Al Annealed Milling 500°C

1.2 Milled annealing cu-al alloy

Fig.1.2 from the optical spectrum Cu-Al nanomaterials consists two main spr peaks a sharp peak in the uv region

around 314 nm for al nanoclusters move to blueshift and a broad peak in the visible move to red shift around cu 570 nm was observed.

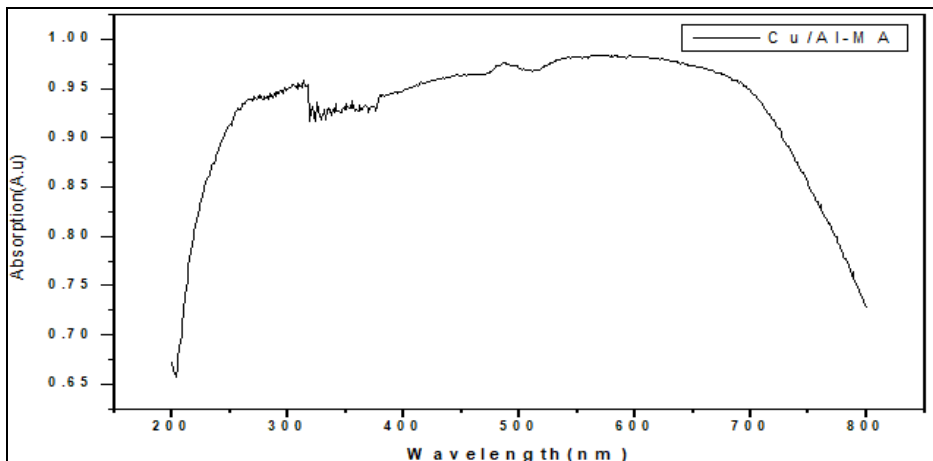


Fig 1.2: Optical absorption spectrum for Cu-Al Milling Annealed. 500°C

1.3 Only annealed Cu-Al alloy

Fig.1.3 from the optical spectrum Cu-Al alloy nanomaterials consists two main spr peaks a sharp peak in the uv region

around 265 nm for al blue shift nanoclusters and a broad peak in the visible move to red shift around cu 694 nm was observed.

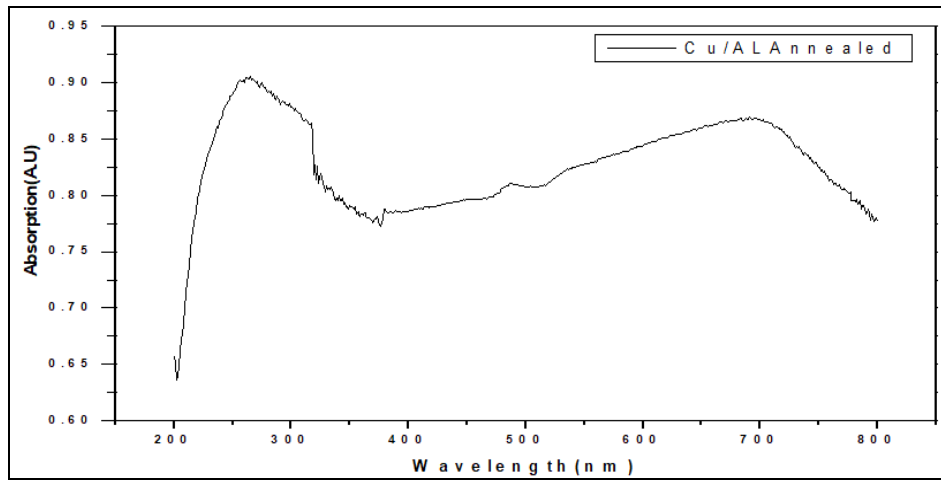


Fig 1.3: Optical absorption spectrum for Cu-Al Only Annealed 500°C

On the comparative studies between the sample which has been annealed on the grind and the sample brought under milled and then heat treated and the surface only annealed. Annealed milling Cu-Al consists two main spr peaks a sharp peak in the uv around 314 nm for al nanoclusters move to blue shift and a broad peak in the visible red shift region around Cu 488 nm was observed. Miiled annealing consists two main spr peaks a sharp peak in the uv around 314 nm for al nanoclusters move to blue shift and a broad peak in the visible red shift around Cu 488 nm was observed. Above two elements small level variations for spr peaks but surface annealed elements has very good move to al blue shift al and move to cu red shift.

1.4 Optical band gap

Copper oxide nano particles (1.2 eV) is indirect band gap^[10,12]. Annealed milled particle size is reduced same time band gap is increased that is show the tauc plot diagram Fig 1.4(a). CuO band gap increased 1.2 eV to 1.25 eV. optical band gap is increased CuO its used to semiconductor device ^[11]. Milled annealed particle size is bulk compare to the annealed milled particle size for the band gap reduced show the tauc plot diagram Fig 1.4(b) 1.2 ev to 1.90 eV^[9]. Only annealed particle size is bulk compare to annealed milled and milled annealed show the tauc plot diagram Fig 1.4(c) band gap size reduced to 1.2 eV to 1.10 eV.

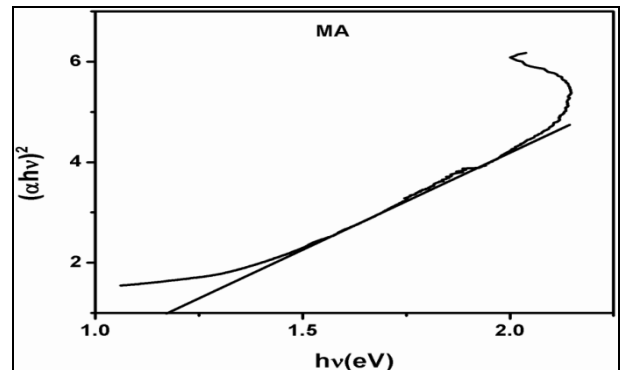


Fig 1.4(b): Optical band gap for Cu-Al Milling Annealed. 500°C

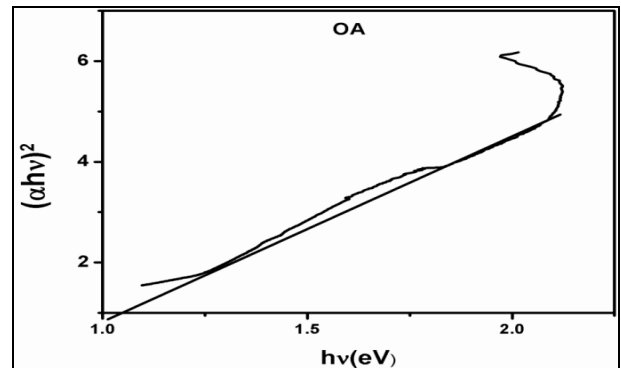


Fig 1.4(c): Optical band gap for Cu-Al Only Annealed 500°C

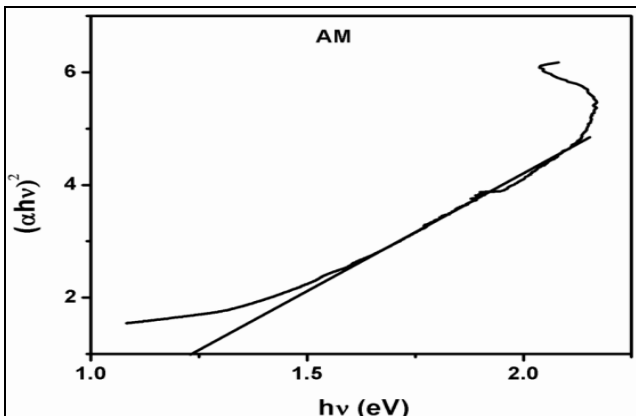


Fig 1.4(a): Optical band gap for Cu-Al Annealed Milling. 500°C

2. SEM (Scanning electron microscopy)

Annealed Milled

The morphology and textural properties of the prepared powders were investigated by scanning electron microscopy (SEM). Figure 2.1, shows the representative SEM micrograph taken for Cu-Al nanoparticles annealed at 500° C for 1h then subjected to high energy ball milled at 250rpm for 1 h. These SEM images exhibits highly agglomerated particles having some voids ^[6]. Images also show that the particles are irregular in shape, with a variation in morphology and the sizes.

The size, shape and texture of the initial as well as nano structured Cu-Al were studied using Secondary Electron Imaging mode of Scanning electron microscopy (SEM).

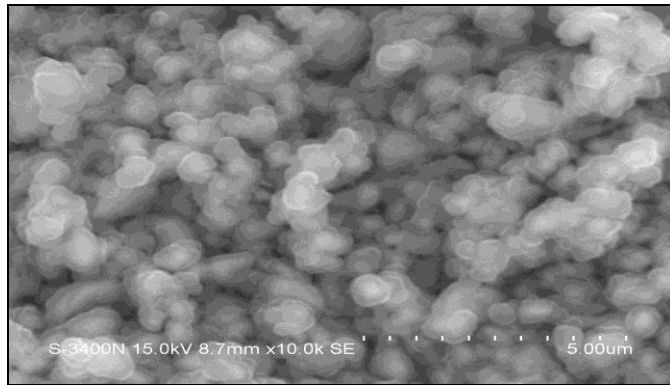


Fig 2.1: Annealed Milled Cu-Al SEM image

Milled Annealed

Figure 2.2, shows the SEM image of initial Cu-Al nanoparticles high energy ball milled at 250rpm for 1 h then subjected to annealed at 500°C for 1h. The initial particles are mostly angular in shape and also having some voids^[7]. It clearly visible the aluminum nanoparticles from the copper nanoparticles. This is may be due to reduced size particle under heat treatment.

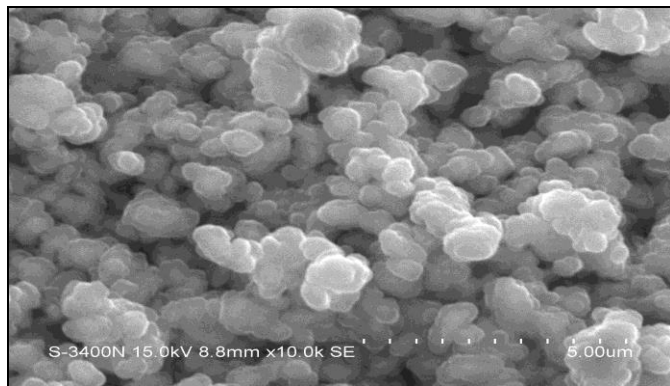


Fig 2.2: Milled Annealed Cu-Al SEM image

3.1 Annealed Milled Cu-Al X-RD

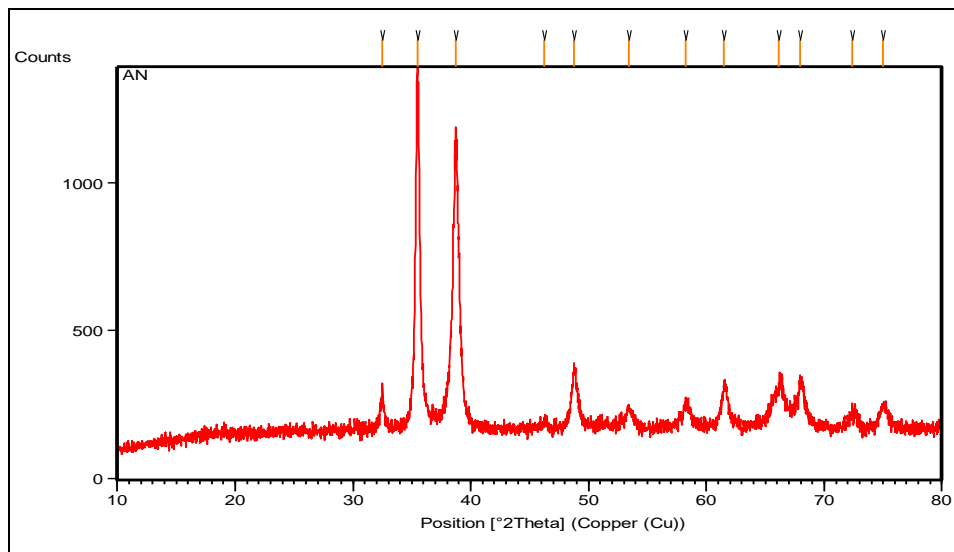


Fig 3.1

Only Annealed

Figure 2.3, shows the SEM image for the morphology and surface texture of an only annealed Cu-Al nanostructured particle shows that the image closely bonded and alloyed and has some smooth surface.

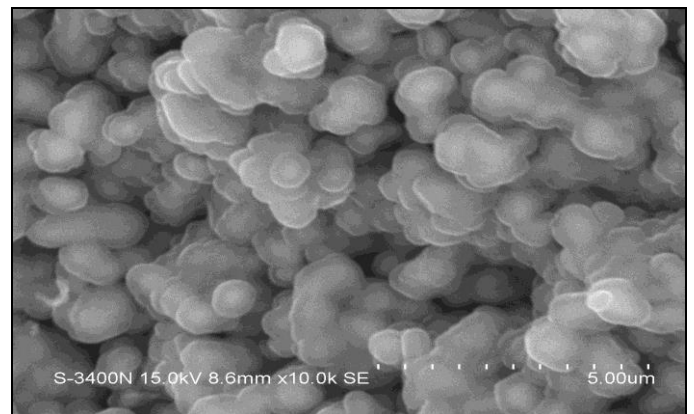


Fig 2.3: Only Annealed Cu-Al SEM image

3. XRD (X-Ray Diffraction)

The crystalline state was determined by powder X-ray diffraction (XRD). Fig.3.1 shows the representative powder XRD pattern for Cu-Al particles annealed at 500° C for 1h then subjected to high energy ball-milled at 250 rpm for 1h^[14]. For comparison the XRD pattern for grind and then annealed Cu-Al is given in Fig. 3.2^[15]. It can be seen from the XRD patterns that the prepared phase is matching well with the Miller indices corresponding to the pure FCC phase of bulk crystalline Cu-Al structure. For the relative calculation of only annealed Cu-Al is given in Fig.3.3. It can be seen from the XRD patterns that the prepared phase is matching well whereas there is a average variation in the peak between the three experimental graph^[6, 7]. But it resembles the same differences in ratio.

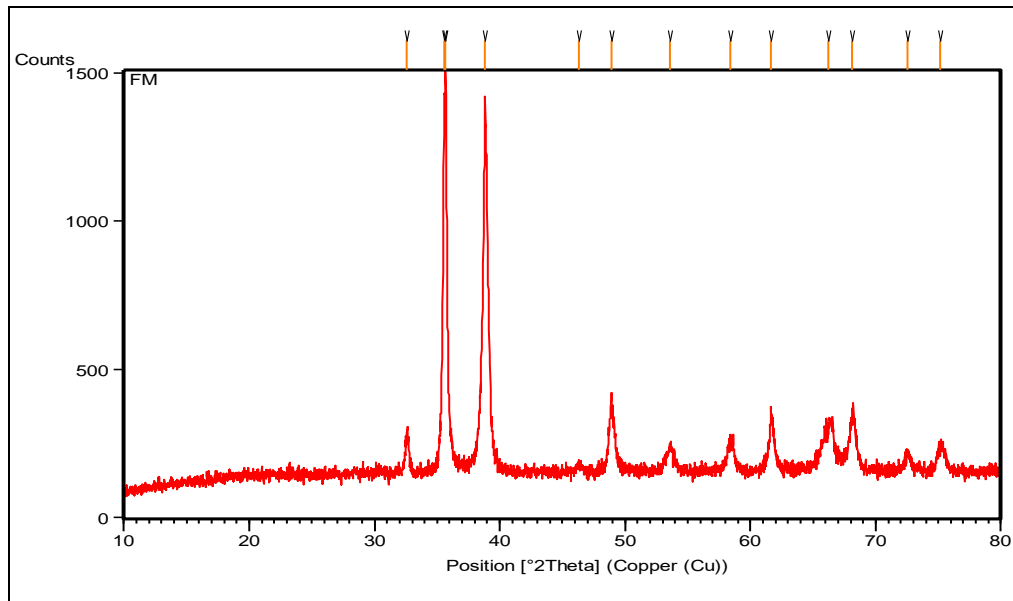


Fig 3.2

3.2 Milled Annealed Cu-Al X-RD

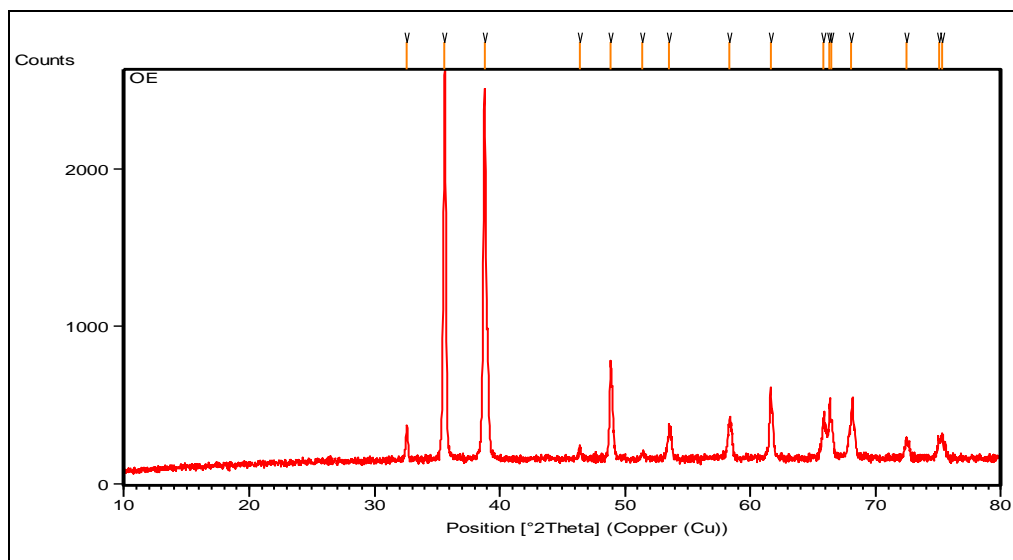


Fig 3.3

3.3 Only Annealed Cu-Al X-RD

The average particle size was calculated from (844) diffraction peak using Scherer's equation: The average crystallite size was calculated from the full width at half maximum (FWHM) of the X-ray diffraction peak using Scherer's equation ^[17].

$$D = (k \lambda) / (B \cos \theta)$$

Where,

D is the particle diameter,

λ is the X – Ray wavelength(0.15418 nm),

B is the FWHM of the diffraction peak,

θ is the diffraction angle and

K- is the Scherer's constant of the order of unity for usual crystals. The average particle size calculated were

approximately 844cts, 659cts, 1751cts for the samples milled at 250 rpm and annealed at 500° C, for AN, FM, and OE respectively. From the above XRD results it has been observed that broadening of the diffraction peaks increases and the peak intensity of the peak is decreases with increasing milling and annealing and its reverse technique ^[13]. This indicates that the particle size decreases with increasing milling and annealing and its reverse technique.

The existence of stress in the materials results in lattice distortions of crystals; consequently, the diffraction peaks of the crystals are broadened.

4. Crystalline Size of CU-AL Nano Particle

Annealed milled Cu-Al from fig (4.1), FWHM increases with decrease the crystalline size ^[16]. Crystalline size decreases in

non-linear manner, it starts from 1.5nm and it reaches 0.18nm. Milled annealed Cu-Al from fig (4.2), FWHM increases with decrease the crystalline size. Crystalline size decreases in linear manner, it starts from 0.7nm and it reaches 0.175nm. Only Annealed Cu-Al from fig (4.3), FWHM increases with decrease the crystalline size [7]. Crystalline size decreases in linear manner, it starts from 1.5nm and it reaches 0.45nm.

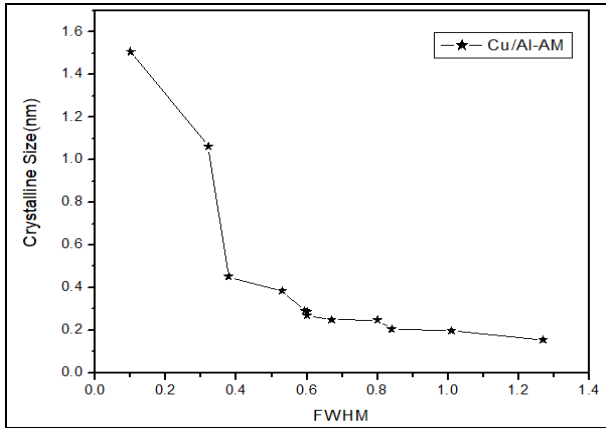


Fig 4.1: FWHM VS Crystalline size Cu-Al annealed milled

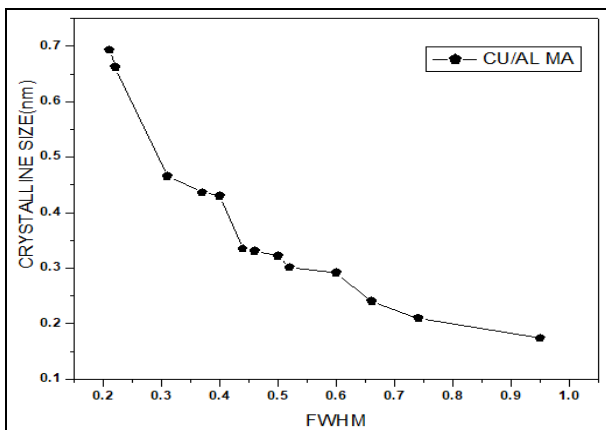


Fig 4.2: FWHM VS Crystalline size Cu-Al milled annealed

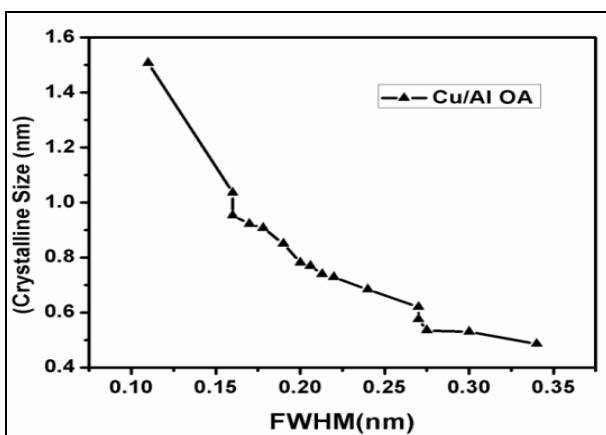


Fig 4.3: FWHM VS crystalline size Cu-Al annealed.

5. Lattice distortion of CuAl_2 nano particle

Annealed milled Cu-Al from fig(5.1), FWHM increases with increases in lattice distortion. The lattice distortion starts

approximately from 0.05 to nearly 0.9. Milled annealed Cu-Al from fig(5.2), FWHM increases with increases in lattice distortion. The lattice distortion starts approximately from 0.05 to nearly 0.65. Only Annealed Cu-Al from fig(5.3), FWHM increases with increases in lattice distortion. The lattice distortion starts approximately from 0.03 to nearly 0.65

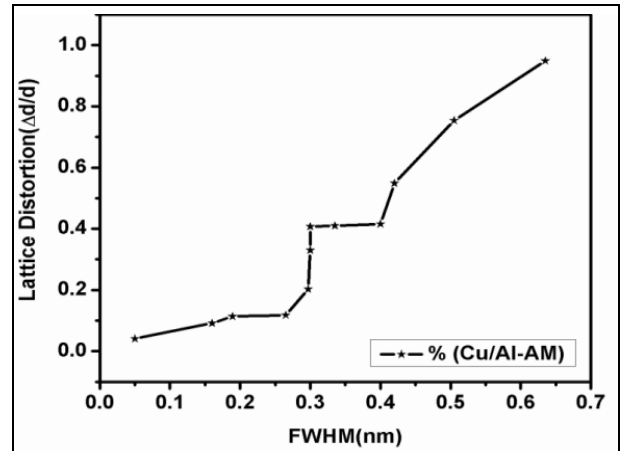


Fig 5.1: FWHM (nm) Vs Lattice distortion ($\Delta d/d$) Cu-Al annealed and milled

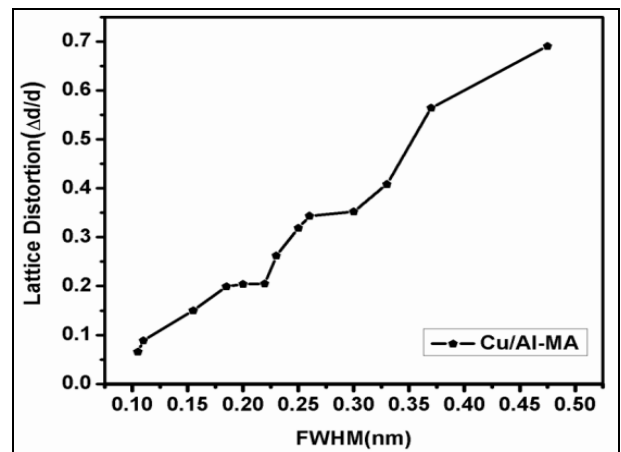


Fig 5.2: FWHM (nm) Vs Lattice distortion ($\Delta d/d$) Cu-Al milled and annealed

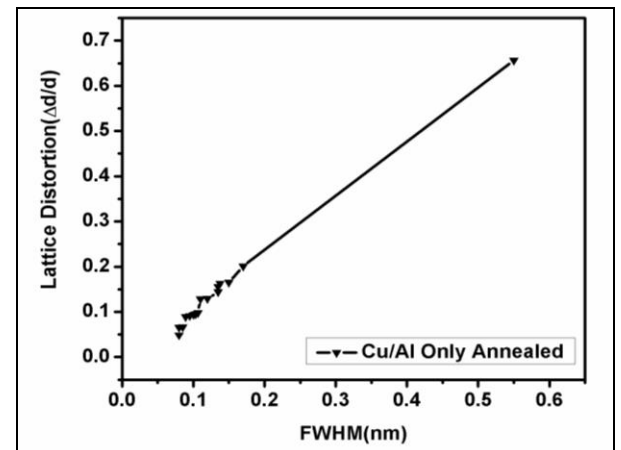


Fig 5.3: FWHM (nm) Vs lattice distortion ($\Delta d/d$) Cu-Al Only Annealed

Conclusions

Cu-Al nano particles were prepared by high energy ball milling technique. There are three types of process using annealed milled, milled annealed and only annealed. Annealed milling process is the best process for reduced the particle grain size compare to the other two process for milled annealing and only annealing. The prepared nanoparticles were characterized for using uv-visible spectroscopy results shows that absorbance spectrum of Cu-Al alloys existence and optical band gap is increased for annealed milled process, scanning electron microscopy results shows that nanoparticles grain size and XRD results show that the prepared nanoparticles retain the crystalline size and lattice distortion.

References

1. Molka Ben Makhlof, Tarek Bachaga, Joan JosepSunol, Mohamed Dammak and Mohamed Khitouni Metals. 2016; 6:145.
2. Gaona-Jimenez S, Rodríguez-Díaz RA, Sedano A, Porcayo-Calderon RA, Ocampo AM, Serna-Barquera S, *et al.* Digest Journal of Nanomaterials and Biostructures. 2017; 12(2):449-462.
3. Jamal NA, Farazila Y, Ramesh S, Anuar Materials H. Research Innovations. 2014; 18:6.
4. Alexandre Nogueira Ottoboni Dias, Aline da Silva, Carlos Alberto Rodrigues, Míriande Lourdes Noronha Motta Melob, Geovani Rodrigues b, Gilbert Silva Materials Research. 2017; 20(3): 747-754.
5. Mitka M, Lity L, Dobrzy A, Góral W. Maziarz Proc. of the International Conference on Mechanochemistry and Mechanical Alloying, Kraków, Poland, 2014.
6. Sujankar, Shweta logad Choudhary, Chiranjithdebnath, Sunilverma, Kunwar Bartwal. Universal journal of materials science. 2013; 1(2):18-24.
7. Baburao J, Catherin GJ, Narasimhamurthy I, Venkatarao D, Nookaraju B. International Journal of engineering, science and technology. 2011; 3(4):82-88.
8. Diwakar Chauhan, Satsangi VR, Sahab Dass, Rohit Shrivastav Bull. Mater. Sci Indian Academy of Sciences. 2006; 29(7):709-716.
9. Wang Y, Lany S, Ghanbaja J, Fagot-Revurat Y, Chen YP, *et al.* Physical Review B Condensedmatter and materials physics, American Physical Society. 2016; 94(24):245418. <10.1103/Phys-RevB.94.245418>. <hal-01430765>
10. Nadir F, Habubi Khudheir, Mishjil Hayfa A, Rashid G, Bassam G. Rasheed IJAP Lett. 2008; 1:1.
11. Mugwang FK, Karimi PK, Njoroge WK, Omayio O, Waita SM. Int. J. Thin Film Sci. Tec. 203; 2(1):15-24.
12. Asha A, Radhakrishnan B. Baskaran Beena, Indian Journal of Advances in Chemical Science. 2014; 2(2):158-161.
13. Cleo Kosanovi, Mirko Stubi, Ana Mu`ic, Nenad Toma. Croatica Chemica acta, CCACAA. 2008; 81(3):431-435, ISSN-0011-1643 CCA-3261.
14. Tcherdyntsev VV, Sviridova TA, Shevchukov AP, Kaloshkin SD. Journal of Physics: Conference Series. 2009, 144 012024.
15. Akbar Salarvand, Vahid Shafi Pour. International Journal of Engineering Science and Technology (IJEST). 2011; 8: ISSN: 0975-5462.
16. Shengqichen, Yanchunzhou. yilij. Mater. sci. Tecnol, 1997, 13.
17. Cullity BD. Elements of X-ray diffraction. 2nd ed. Addison-Wesley, Reading, Mass, 1978.